



Search for the Σ^* state in $\Lambda_c^+ \rightarrow \pi^+ \pi^0 \pi^- \Sigma^+$ decay by triangle singularity

Ju-Jun Xie^{a,*}, Eulogio Oset^b

^a Institute of Modern Physics, Chinese Academy of Sciences, Lanzhou 730000, China

^b Departamento de Física Teórica and IFIC, Centro Mixto Universidad de Valencia-CSIC, Institutos de Investigación de Paterna, Aptdo. 22085, 46071 Valencia, Spain



ARTICLE INFO

Article history:

Received 29 November 2018
Accepted 4 April 2019
Available online 9 April 2019
Editor: W. Haxton

ABSTRACT

A Σ^* resonance with spin-parity $J^P = 1/2^-$ and mass in the vicinity of the $\bar{K}N$ threshold has been predicted in the unitary chiral approach and inferred from the analysis of CLAS data on the $\gamma p \rightarrow K^+ \pi^0 \Sigma^0$ reaction. In this work, based on the dominant Cabibbo favored weak decay mechanism, we perform a study of $\Lambda_c^+ \rightarrow \pi^+ \pi^0 \Sigma^*$ with the possible Σ^* state decaying into $\pi^- \Sigma^+$ through a triangle diagram. This process is initiated by $\Lambda_c^+ \rightarrow \pi^+ \bar{K}^* N$, then the \bar{K}^* decays into $\bar{K} \pi$ and $\bar{K} N$ produce the Σ^* through a triangle loop containing $\bar{K}^* N \bar{K}$ which develops a triangle singularity. We show that the $\pi^- \Sigma^+$ state is generated from final state interaction of $\bar{K} N$ in S -wave and isospin $I = 1$, and the $\Lambda_c^+ \rightarrow \pi^+ \pi^0 \pi^- \Sigma^+$ decay can be used to study the possible Σ^* state around the $\bar{K} N$ threshold. The proposed decay mechanism can provide valuable information on the nature of the Σ^* resonance and can in principle be tested by facilities such as LHCb, BelleII and BESIII.

© 2019 The Authors. Published by Elsevier B.V. This is an open access article under the CC BY license (<http://creativecommons.org/licenses/by/4.0/>). Funded by SCOAP³.

1. Introduction

Investigating low-lying excited states of $\Sigma(1193)$, Σ^* , with isospin $I = 1$ and strangeness $S = -1$ is one of the important issues in hadronic physics [1–3]. The Σ^* states were mostly produced and studied in antikaon-nucleon reactions, and the information on their properties is still rather limited [3]. Based on the chiral unitary approach, the low-lying $S = -1$ excited baryons were studied by means of coupled channels in Refs. [4–15]. In addition to the well reproduced properties of the $\Lambda(1405)$, a possible resonance-like structure in $I = 1$ around the $\bar{K}N$ threshold was found in Ref. [6] as a bound state and in Ref. [10] as a strong cusp effect. Then it was further investigated in Ref. [16] based on the analysis of the experimental data on the $\gamma p \rightarrow K^+ \pi^\pm \Sigma^\mp$ reactions [17,18]. Such a state near the $\bar{K}N$ threshold is also discussed in Refs. [11,12], while in Ref. [15], a Σ^* state is found with mass around 1400 MeV, though it is not clear if it is related to one or two poles in the complex plane. On the other hand, the effect of this possible $\bar{K}N$ state with mass about 1430 MeV in the processes of $\chi_{c0}(1P) \rightarrow \pi \bar{\Sigma} \Sigma$ (Λ) decays was also studied in Refs. [19,20].

The nonleptonic weak decays of charmed baryons, particularly Λ_c^+ decays into two mesons and one baryon, have shown a great value to produce baryonic resonances with $S = -1$ and learn about their nature [21–24]. In some cases the production rate is enhanced by the presence of a triangle singularity (TS) in the reaction mechanism [25,26]. The TS appears from a loop diagram in the decay of a particle 1 into two particles 2 and 3 through the following process: at first the particle 1 decays into particles A and B, and the particle A subsequently decays into particles 2 and C, and finally the particles B and C merge and form the particle 3 in the final state.

Following the work of Ref. [26], in this paper, we focus on the $\Lambda_c^+ \rightarrow \pi^+ \pi^0 \pi^- \Sigma^+$ decay taking into account the $\pi^- \Sigma^+$ final state interaction from the triangle diagram. We consider the external W^+ emission diagram for the transition of Λ_c^+ into $\pi^+ \bar{K}^* N$, which gives the main contribution to the $\Lambda_c^+ \rightarrow \pi^+ \pi^0 \pi^- \Sigma^+$ process [26]. Since we take into account the external W^+ emission diagram, the W^+ produces the π^+ in one vertex and in the other one includes a $c \rightarrow s$ transition. Then we have a π^+ and an sud cluster, with the ud diquark in $I = 0$, because there these quarks are spectators. Hence the sud cluster hadronizes in $\bar{K}^* N$ in $I = 0$, and, since π has isospin 1, the $\pi \Sigma$ system should be also in isospin 1 to keep the isospin conserved. We will show that the production of the $\bar{K}N$ state is enhanced by the TS in the $\pi^0 \pi^- \Sigma^+$ mass distribution, and that a narrow peak or cusp structure around

* Corresponding author.

E-mail addresses: xiejjun@impcas.ac.cn (J.-J. Xie), oset@ific.uv.es (E. Oset).

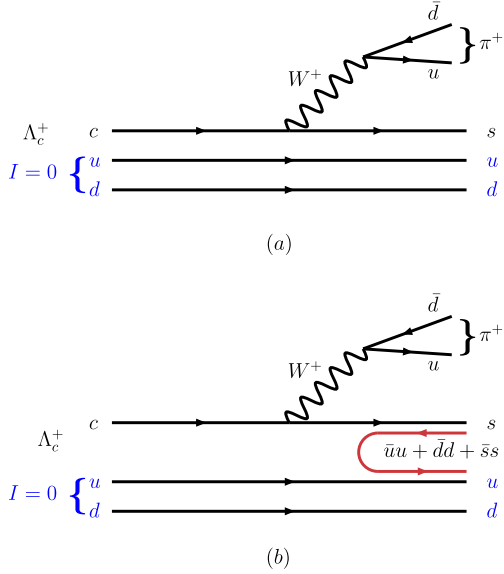


Fig. 1. (a) Quark level diagram for $\Lambda_c^+ \rightarrow \pi^+ sud$. (b) Hadronization through $\bar{q}q$ creation with vacuum quantum numbers.

the $\bar{K}N$ threshold in the $\pi\Sigma$ mass distribution appears. The observation of the TS in this process would give further support to the existence of the $\bar{K}N$ resonance,¹ and provide us better understanding on the triangle singularity.

This article is organized as follows. In Sec. 2, we present the theoretical formalism for calculating the decay amplitude of $\Lambda_c^+ \rightarrow \pi^+ \pi^0 \pi^- \Sigma^+$. Numerical results and discussions are presented in Sec. 3, followed by a summary in the last section.

2. Formalism

We consider the external emission mechanism of Fig. 1. The mechanism is Cabibbo favored. In Fig. 1 (a) we see that the original ud quarks of the Λ_c^+ are in $I=0$ and furthermore they are spectators in the reaction, hence they continue to have $I=0$ in the final sud state. This state hadronizes to meson-baryon pairs after creating a $\bar{q}q$ pair with the quantum numbers of the vacuum. In our case we are interested in the \bar{K}^*N production. The insertion of $\bar{q}q$ can be done between any two quarks, but in our case it must involve the strange quark. The reason is that we want to have \bar{K}^*N in S -wave, hence negative parity. Since the ud quarks are spectators and have positive parity, it must be the strange quark that is produced in $L=1$. But we want it in its ground state in the \bar{K}^* after the hadronization, hence it has to be involved in the hadronization process.

The explicit flavor combination of meson and baryon pairs of the hadronization [see the process shown in Fig. 1 (b)], H , is shown in Ref. [26] and one finds,

$$H = K^{*-} p + \bar{K}^{*0} n - \frac{\sqrt{6}}{3} \phi \Lambda, \quad (1)$$

and one ignores the $\phi\Lambda$ component that has no role in the TS mechanism. We can see that H in Eq. (1) has $I=0$, since $(\bar{K}^{*0}, -K^{*-})$ is our isospin doublet. This corresponds to the isospin of $s(ud)_{I=0}$ just after the weak vertex, which is conserved after that.

Once $\pi^+ \bar{K}^*N$ is produced, the \bar{K}^* decays to $\pi\bar{K}$ and the $\bar{K}N$ interact to give $\pi\Sigma$. Since \bar{K}^*N is in $I=0$, so must be the $\pi\pi\Sigma$

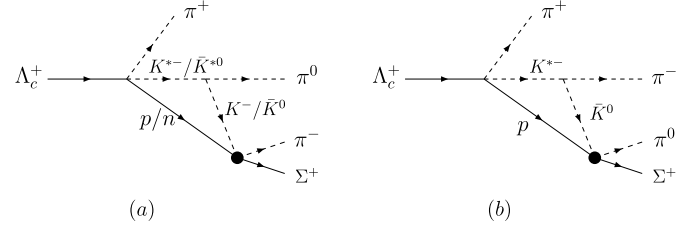


Fig. 2. Triangle diagrams for the decay of $\Lambda_c^+ \rightarrow \pi^+ \pi^0 \pi^- \Sigma^+$. (a) represents the final state interaction of $\bar{K}N \rightarrow \pi^- \Sigma^+$, while (b) represents the final state interaction of $\bar{K}^0 p \rightarrow \pi^0 \Sigma^+$. The black ‘dot’ stands for the vertex of the final state interaction of $\bar{K}N \rightarrow \pi\Sigma$ in S -wave.

system, which forces the $\pi\Sigma$ system, coming from the $\bar{K}N$ interaction, to have $I=1$ if there is isospin conservation, as we shall assume here. This is shown in Fig. 2.

By filtering the $I=1$ $\pi\Sigma$ system, the $\bar{K}N \rightarrow \pi\Sigma$ amplitude incorporates the $\Sigma^*(1430)$ resonance and we should see the signal of the state clearly in the $\pi\Sigma$ mass distribution. In addition, as we shall see, the mechanism develops a TS which enhances the production of the $\Sigma^*(1430)$ state. In Fig. 2 we have separated the two possible decay modes: Fig. 2 (a) shows the contribution from the final state interaction of $\bar{K}^*N \rightarrow \pi^- \Sigma^+$, while Fig. 2 (b) stands for the transition of $\bar{K}^0 p \rightarrow \pi^0 \Sigma^+$.

We first consider the decay of $\Lambda_c^+ \rightarrow \pi^+ K^{*-} p$, proceeding via S -wave, and we take the decay amplitude as [26],

$$t_{\Lambda_c^+ \rightarrow \pi^+ K^{*-} p} = A \vec{\sigma} \cdot \vec{\epsilon}, \quad (2)$$

with A constant. Then we can easily obtain the branching ratio $Br(\Lambda_c^+ \rightarrow \pi^+ K^{*-} p)$, summing over the \bar{K}^{*-} polarizations, as

$$Br(\Lambda_c^+ \rightarrow \pi^+ K^{*-} p) = \frac{3m_N |A|^2}{8\pi^3 M_{\Lambda_c^+} \Gamma_{\Lambda_c^+}} \times \int_{m_{K^{*-}+m_p}}^{M_{\Lambda_c^+}-m_{\pi^+}} p_{\pi^+} \tilde{p}_{K^{*-}} dM_{K^{*-}p}, \quad (3)$$

where p_{π^+} is the momentum of π^+ in the Λ_c^+ rest frame, and $\tilde{p}_{K^{*-}}$ is the momentum of \bar{K}^* in the $K^{*-}p$ rest frame with invariant mass $M_{K^{*-}p}$,

$$p_{\pi^+} = \frac{\lambda^{1/2}(M_{\Lambda_c^+}^2, m_{\pi^+}^2, M_{K^{*-}p}^2)}{2M_{\Lambda_c^+}}, \quad (4)$$

$$\tilde{p}_{K^{*-}} = \frac{\lambda^{1/2}(M_{K^{*-}p}^2, m_{K^{*-}}^2, m_p^2)}{2M_{K^{*-}p}}, \quad (5)$$

with $\lambda(x, y, z)$ the ordinary Källén function.

By calculating the partial decay width of $\Lambda_c^+ \rightarrow \pi^+ K^{*-} p$, using the experimental branching ratio of $Br(\Lambda_c^+ \rightarrow \pi^+ K^{*-} p) = (1.4 \pm 0.5) \times 10^{-2}$ and $\Gamma_{\Lambda_c^+} = (3.3 \pm 0.1) \times 10^{-9}$ MeV [3], we can determine the value of the constant $|A|^2$,

$$|A|^2 = (3.9 \pm 1.4) \times 10^{-16} \text{ MeV}^{-2}, \quad (6)$$

where the error is taken from the experimental error in the branching ratio of $Br(\Lambda_c^+ \rightarrow \pi^+ K^{*-} p)$. In view of the weights in H in Eq. (1), the same value of $|A|^2$ is used for the decay of $\Lambda_c^+ \rightarrow \pi^+ \bar{K}^{*0} n$.

Next, we write the total decay amplitude of $\Lambda_c^+ \rightarrow \pi^+ \pi^0 \pi^- \Sigma^+$ for those diagrams shown in Fig. 2,²

¹ In the following, we use $\Sigma^*(1430)$ to denote the $\bar{K}N$ resonance.

² More details can be found in Ref. [26].

$$t_{\text{total}} = -\frac{Ag}{\sqrt{2}} \left(\vec{\sigma} \cdot \vec{k}_a t_T^a \mathcal{M}^a + \sqrt{2} \vec{\sigma} \cdot \vec{k}_b t_T^b \mathcal{M}^b \right), \quad (7)$$

where \vec{k}_a and \vec{k}_b are the momenta of the π^0 and π^- in the diagrams of Fig. 2 (a) and (b), respectively, calculated in the $\pi^0\pi^-\Sigma^+$ rest frame, and the coupling g is given by $g = m_V/2f_\pi$ with $m_V = 780$ MeV and $f_\pi = 93$ MeV. In Eq. (7), \mathcal{M}^a and \mathcal{M}^b are the two-body scattering amplitudes, which depend on the invariant masses of $M_{\pi^-\Sigma^+}$ and $M_{\pi^0\Sigma^+}$, respectively, and they have the explicitly forms as,

$$\mathcal{M}^a = t_{K^-p \rightarrow \pi^-\Sigma^+} - t_{\bar{K}^0 n \rightarrow \pi^-\Sigma^+}, \quad (8)$$

$$\mathcal{M}^b = t_{\bar{K}^0 p \rightarrow \pi^0\Sigma^+}, \quad (9)$$

where $t_{K^-p \rightarrow \pi^-\Sigma^+}$ and $t_{\bar{K}^0 n \rightarrow \pi^-\Sigma^+}$ depend on $M_{\pi^-\Sigma^+}$, and $t_{\bar{K}^0 p \rightarrow \pi^0\Sigma^+}$ depends on $M_{\pi^0\Sigma^+}$. The factor $\sqrt{2}$ in Eq. (7) and the minus sign in Eq. (8) have their origin in the different $\bar{K}^* \rightarrow \pi K$ vertices. Note that the two combinations, $K^-p - \bar{K}^0 n$ and $\bar{K}^0 p$ have $I = 1$, as it should be.

In addition, we give explicitly the amplitude t_T^a for the case of K^{*-} , p and K^- in the triangle loop, as an example,

$$\begin{aligned} t_T^a &= \int \frac{d^3q}{(2\pi)^3} \frac{m_p}{2\omega_{K^*} - \omega_p \omega_{K^-}} \frac{1}{k_a^0 - \omega_{K^-} - \omega_{K^*} + i\frac{\Gamma_{K^*}}{2}} \\ &\times \frac{1}{P^0 + \omega_p + \omega_{K^-} - k_a^0} \left(2 + \frac{\vec{q} \cdot \vec{k}_a}{|\vec{k}_a|^2} \right) \\ &\times \frac{P^0 \omega_p + k_a^0 \omega_{K^-} - (\omega_p + \omega_{K^-})(\omega_p + \omega_{K^-} + \omega_{K^*})}{P^0 - \omega_{K^*} - \omega_p + i\frac{\Gamma_{K^*}}{2}} \\ &\times \frac{1}{P^0 - \omega_p - \omega_{K^-} - k_a^0 + i\epsilon}, \end{aligned} \quad (10)$$

with $P^0 = M_{\pi^-\pi^0\Sigma^+}$ the invariant mass of the final $\pi^0\pi^-\Sigma^+$ system, $\omega_p = \sqrt{|\vec{q}|^2 + m_p^2}$, $\omega_{K^-} = \sqrt{|\vec{q} + \vec{k}_a|^2 + m_{K^-}^2}$, and $\omega_{K^*} = \sqrt{|\vec{q}|^2 + m_{K^*}^2}$. The energy k_a^0 and momentum $|\vec{k}_a|$ of π^0 emitted from K^{*-} are given by

$$k_a^0 = \frac{M_{\pi^-\pi^0\Sigma^+}^2 + m_{\pi^0}^2 - M_{\pi^-\Sigma^+}^2}{2M_{\pi^-\pi^0\Sigma^+}}, \quad (11)$$

$$|\vec{k}_a| = \sqrt{(k_a^0)^2 - m_{\pi^0}^2}. \quad (12)$$

While, k_b^0 , $|\vec{k}_b|$, and t_T^b can easily be obtained just applying the substitution to k_a^0 , $|\vec{k}_a|$ and t_T^a with $m_{\pi^0} \rightarrow m_{\pi^-}$ and $M_{\pi^-\Sigma^+} \rightarrow M_{\pi^0\Sigma^+}$.

Then we obtain the final invariant masses distribution for four particles in the final state,

$$\begin{aligned} \frac{d^3\Gamma}{dM_{\pi^0\pi^-\Sigma^+} dM_{\pi^-\Sigma^+} dM_{\pi^0\Sigma^+}} &= \frac{g^2 |A|^2 m_{\Sigma^+}}{128\pi^5 M_{\Lambda_c^+}} \tilde{p}_{\pi^+} \\ &\times \frac{M_{\pi^-\Sigma^+} + M_{\pi^0\Sigma^+}}{M_{\pi^0\pi^-\Sigma^+}} \left(|\vec{k}_a|^2 |t_T^a \mathcal{M}^a|^2 + 2|\vec{k}_b|^2 |t_T^b \mathcal{M}^b|^2 \right. \\ &\left. + 2\sqrt{2} \text{Re}[t_T^a \mathcal{M}^a (t_T^b \mathcal{M}^b)^*] \vec{k}_a \cdot \vec{k}_b \right), \end{aligned} \quad (13)$$

with

$$\tilde{p}_{\pi^+} = \frac{\lambda^{1/2}(M_{\Lambda_c^+}^2, M_{\pi^0\pi^-\Sigma^+}^2, m_{\pi^+}^2)}{2M_{\Lambda_c^+}}. \quad (14)$$

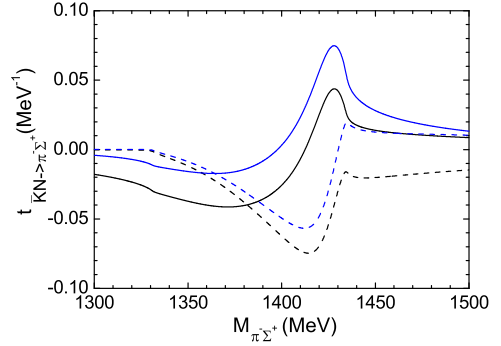


Fig. 3. Transition amplitudes of $\bar{K}N \rightarrow \pi^-\Sigma^+$ in S-wave.

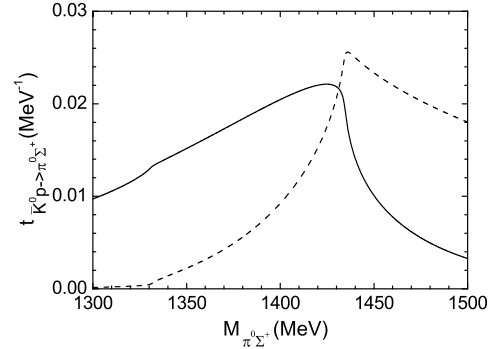


Fig. 4. Transition amplitudes of $\bar{K}^0 p \rightarrow \pi^0\Sigma^+$ in S-wave.

In Eq. (13), $\vec{k}_a \cdot \vec{k}_b$ is evaluated in terms of $M_{\pi^0\pi^-\Sigma^+}$, $M_{\pi^-\Sigma^+}$, and $M_{\pi^0\Sigma^+}$,

$$\vec{k}_a \cdot \vec{k}_b = \frac{m_{\pi^0}^2 + m_{\pi^-}^2 - M_{\pi^0\pi^-}^2 + 2k_a^0 k_b^0}{2}, \quad (15)$$

with

$$\begin{aligned} M_{\pi^0\pi^-}^2 &= M_{\pi^0\pi^-\Sigma^+}^2 + m_{\pi^0}^2 + m_{\pi^-}^2 + m_{\Sigma^+}^2 \\ &\quad - M_{\pi^-\Sigma^+}^2 - M_{\pi^0\Sigma^+}^2. \end{aligned} \quad (16)$$

On the other hand, we have to regularize the integral in Eq. (10). In this work, we use the same cutoff of the meson loop that is used to calculate $t_{K^-p \rightarrow \pi^-\Sigma^+}$ with $\theta(q_{\text{max}} - |\vec{q}^*|)$, where \vec{q}^* is the \vec{q} momentum in the R rest frame (see Ref. [27] for more details).

3. Numerical results

In Figs. 3 and 4 the two body transition amplitudes of $\bar{K}N \rightarrow \pi\Sigma$ are shown. We plot the real and imaginary parts of those two body transition amplitudes. In Fig. 3, the blue curve and solid curve stand for the real parts of $t_{K^-p \rightarrow \pi^-\Sigma^+}$ and $t_{\bar{K}^0 n \rightarrow \pi^-\Sigma^+}$, respectively, while the blue-dashed curve and dashed curve stand for the imaginary parts of $t_{K^-p \rightarrow \pi^-\Sigma^+}$ and $t_{\bar{K}^0 n \rightarrow \pi^-\Sigma^+}$, respectively. In Fig. 4, the solid and dashed curves are the real and imaginary parts of $t_{\bar{K}^0 p \rightarrow \pi^0\Sigma^+}$, respectively. It can be observed that the $\text{Re}(t_{\bar{K}N \rightarrow \pi^-\Sigma^+})$ have peaks around 1430 MeV, and $|\text{Im}(t_{\bar{K}N \rightarrow \pi^-\Sigma^+})|$ have peaks around 1420 MeV, and there are bump structures for $\text{Re}(t_{\bar{K}^0 p \rightarrow \pi^0\Sigma^+})$ and $\text{Im}(t_{\bar{K}^0 p \rightarrow \pi^0\Sigma^+})$ around 1430 and 1440 MeV, respectively. These results, shown in Figs. 3 and 4, are obtained using the Bethe-Salpeter equation, with the tree level potentials given in Ref. [5]. The loop functions for the intermediate states are regularized using the cutoff method with a cutoff of 630 MeV. This parameter is also used to evaluate the loop integral in the diagrams of Fig. 2.

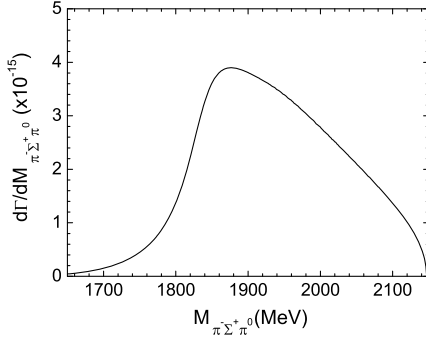


Fig. 5. Invariant $\pi^0\pi^-\Sigma^+$ mass distribution of $\Lambda_c^+ \rightarrow \pi^+\pi^0\pi^-\Sigma^+$ decay.

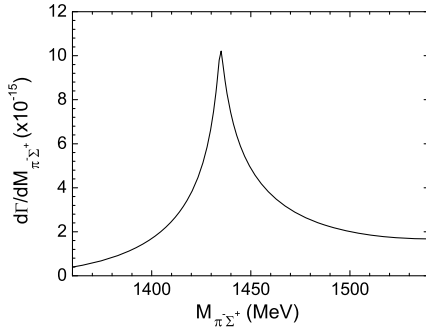


Fig. 6. Invariant $\pi^-\Sigma^+$ mass distribution of $\Lambda_c^+ \rightarrow \pi^+\pi^0\pi^-\Sigma^+$ decay.

With all the ingredients obtained above, one can easily obtain $d\Gamma/dM_{\pi^0\pi^-\Sigma^+}$ by integrating over $M_{\pi^-\Sigma^+}$ and $M_{\pi^0\Sigma^+}$ and using $|A|^2 = 3.9 \times 10^{-16} \text{ MeV}^{-2}$. We show the theoretical results of $d\Gamma/dM_{\pi^0\pi^-\Sigma^+}$ in Fig. 5. We see a clear bump structure of the invariant $\pi^0\pi^-\Sigma^+$ mass distribution around 1880 MeV for $\Lambda_c^+ \rightarrow \pi^+\pi^0\pi^-\Sigma^+$ decay, which is due to the triangle singularity of the triangle diagrams as shown in Fig. 2.

On the other hand, by integrating over $M_{\pi^0\pi^-\Sigma^+}$ and $M_{\pi^0\Sigma^+}$, we obtain $d\Gamma/dM_{\pi^-\Sigma^+}$ which is shown in Fig. 6. We see a really narrow peak of the invariant $\pi^-\Sigma^+$ mass distribution around 1434 MeV for $\Lambda_c^+ \rightarrow \pi^+\pi^0\pi^-\Sigma^+$ decay, which is the contribution from the $\bar{K}N$ resonance which is discussed above. Similar results can be also obtained for $d\Gamma/dM_{\pi^0\Sigma^+}$.

From these results shown in Figs. 5 and 6, one can easily obtain the branching ratio of $Br(\Lambda_c^+ \rightarrow \pi^+\pi^0\pi^-\Sigma^+)$ is about $(3 \pm 1) \times 10^{-4}$, with the error that is taken from the error in $|A|^2$.

One should stress the most remarkable feature in the distributions of Fig. 6: the width of the $\Sigma^*(1430)$ produced is about 10 MeV, remarkably smaller than the other Σ^* resonances of 30 MeV or even bigger [3]. Yet, as discussed in Ref. [16] the peak corresponds to a cusp at the $\bar{K}N$ mass threshold, however, very pronounced. The dynamics of these cusps corresponds to a state nearly bound. Theoretically, a small change in the parameters makes a pole appear. This situation is very similar to the one of the $a_0(980)$ resonance, which both theoretically [28] and experimentally [29] appears as a very pronounced cusp.

4. Conclusions

The triangle singularities have recently shown to be very important in many hadronic decays. In this work we provide the first evaluation of the $\Sigma^*(1430)$ production in the decay of $\Lambda_c^+ \rightarrow \pi^+\pi^0\pi^-\Sigma^+$. The decay mechanism for the production is given by a first decay of the Λ_c^+ into $\pi^+\bar{K}^*N$, then the \bar{K}^* decays into $\bar{K}\pi$ and the $\bar{K}N$ merge to produce the $\Sigma^*(1430)$ through both the final state interaction of $\bar{K}N \rightarrow \pi\Sigma$ transition and a triangle loop con-

taining $\bar{K}^*N\bar{K}$, which develops a singularity of the invariant mass of $\pi^0\pi^-\Sigma^+$ system around 1880 MeV.

It is found that a narrow peak, of the order of 10 MeV, tied to the $\Sigma^*(1430)$ state appears in the final $\pi^-\Sigma^+$ mass spectrum at the energy around the $\bar{K}N$ mass threshold of 1434 MeV. The line shape obtained here is intimately tied to the nature of the $\Sigma^*(1430)$ as a dynamically generated resonance from the meson baryon interaction, and shows up as a cusp structure. The theoretical calculations done here together with the experimental measurements would thus bring valuable information on the nature of this resonance. Corresponding experimental measurements could in principle be done by BESIII [30] and BelleII [31] Collaborations. In this sense the branching ratios obtained here for this $\Sigma^*(1430)$ signal are of the order of 10^{-4} , which are well within the measurable range in these facilities. In view of that, the measurements of the $\Lambda_c^+ \rightarrow \pi^+\pi^0\pi^-\Sigma^+$ decay is strongly encouraged. Besides, the mechanism studied in this work contributes also to the processes of $\Lambda_c^+ \rightarrow \pi^+\pi^0\pi^0\Lambda$ and $\Lambda_c^+ \rightarrow \pi^+\pi^+\pi^-\Lambda$, and thus these processes are also very interesting and can be measured by future experiments.

Acknowledgements

This work is partly supported by the National Natural Science Foundation of China under Grant Nos. 11475227 and 11735003, and by the Youth Innovation Promotion Association CAS (No. 2016367). It is also partly supported by the Spanish Ministerio de Economía y Competitividad and European FEDER funds under the contract number FIS2011-28853-C02-01, FIS2011-28853-C02-02, FIS2014-57026-REDT, FIS2014-51948-C2-1-P, and FIS2014-51948-C2-2-P, and the Generalitat Valenciana in the program Prometeo II-2014/068 (EO).

References

- [1] E. Klempt, J.M. Richard, *Rev. Mod. Phys.* **82** (2010) 1095.
- [2] V. Crede, W. Roberts, *Rep. Prog. Phys.* **76** (2013) 076301.
- [3] M. Tanabashi, et al., Particle Data Group, *Phys. Rev. D* **98** (2018) 030001.
- [4] N. Kaiser, P.B. Siegel, W. Weise, *Nucl. Phys. A* **594** (1995) 325.
- [5] E. Oset, A. Ramos, *Nucl. Phys. A* **635** (1998) 99.
- [6] J.A. Oller, U.G. Meißner, *Phys. Lett. B* **500** (2001) 263.
- [7] E. Oset, A. Ramos, C. Bennhold, *Phys. Lett. B* **527** (2002) 99, Erratum: *Phys. Lett. B* **530** (2002) 260.
- [8] M.F.M. Lutz, E.E. Kolomeitsev, *Nucl. Phys. A* **700** (2002) 193.
- [9] C. Garcia-Recio, J. Nieves, E. Ruiz Arriola, M.J. Vicente Vacas, *Phys. Rev. D* **67** (2003) 076009.
- [10] D. Jido, J.A. Oller, E. Oset, A. Ramos, U.G. Meißner, *Nucl. Phys. A* **725** (2003) 181.
- [11] J.A. Oller, *Eur. Phys. J. A* **28** (2006) 63.
- [12] Z.H. Guo, J.A. Oller, *Phys. Rev. C* **87** (2013) 035202.
- [13] T. Hyodo, D. Jido, *Prog. Part. Nucl. Phys.* **67** (2012) 55.
- [14] Y. Kamiya, K. Miyahara, S. Ohnishi, Y. Ikeda, T. Hyodo, E. Oset, W. Weise, *Nucl. Phys. A* **954** (2016) 41.
- [15] K.P. Khemchandani, A. Martínez Torres, J.A. Oller, arXiv:1810.09990 [hep-ph].
- [16] L. Roca, E. Oset, *Phys. Rev. C* **88** (2013) 055206.
- [17] K. Moriya, et al., CLAS Collaboration, *Phys. Rev. C* **87** (2013) 035206.
- [18] K. Moriya, et al., CLAS Collaboration, *Phys. Rev. C* **88** (2013) 045201, Addendum: *Phys. Rev. C* **88** (2013) 049902.
- [19] E. Wang, J.J. Xie, E. Oset, *Phys. Lett. B* **753** (2016) 526.
- [20] L.J. Liu, E. Wang, J.J. Xie, K.L. Song, J.Y. Zhu, *Phys. Rev. D* **98** (2018) 114017.
- [21] T. Hyodo, M. Oka, *Phys. Rev. C* **84** (2011) 035201.
- [22] K. Miyahara, T. Hyodo, E. Oset, *Phys. Rev. C* **92** (2015) 055204.
- [23] J.J. Xie, L.S. Geng, *Eur. Phys. J. C* **76** (2016) 496.
- [24] J.J. Xie, L.S. Geng, *Phys. Rev. D* **95** (2017) 074024.
- [25] J.J. Xie, F.K. Guo, *Phys. Lett. B* **774** (2017) 108.
- [26] L.R. Dai, R. Pavao, S. Sakai, E. Oset, *Phys. Rev. D* **97** (2018) 116004.
- [27] M. Bayar, F. Aceti, F.K. Guo, E. Oset, *Phys. Rev. D* **94** (2016) 074039.
- [28] J.A. Oller, E. Oset, *Nucl. Phys. A* **620** (1997) 438, Erratum: *Nucl. Phys. A* **652** (1999) 407.
- [29] M. Ablikim, et al., BESIII Collaboration, *Phys. Rev. D* **95** (2017) 032002.
- [30] M. Ablikim, et al., BESIII Collaboration, *Phys. Rev. Lett.* **116** (2016) 052001.
- [31] S.B. Yang, et al., Belle Collaboration, *Phys. Rev. Lett.* **117** (2016) 011801.